

# Potentialiation by Nitric Oxide of Cyclosporin A and FK506-Induced Apoptosis in Renal Proximal Tubule Cells

SONSOLES HORTELANO,\* MANUELA CASTILLA,<sup>†</sup> ANA M. TORRES,<sup>†</sup>  
ALBERTO TEJEDOR,<sup>†</sup> and LISARDO BOSCA<sup>\*</sup>

*\*Institute of Biochemistry (CSIC-UCM), Faculty of Pharmacy, Complutense University, and <sup>†</sup>Experimental Medicine and Surgery Unit, Gregorio Marañón University General Hospital, Madrid, Spain.*

**Abstract.** Proximal tubular epithelial cells (PTEC) exhibit a high sensitivity to undergo apoptosis in response to proinflammatory stimuli and immunosuppressors and participate in the onset of several renal diseases. This study examined the expression of inducible nitric oxide (NO) synthase after challenge of PTEC with bacterial cell wall molecules and inflammatory cytokines and analyzed the pathways that lead to apoptosis in these cells by measuring changes in the mitochondrial transmembrane potential and caspase activation. The data show that the apoptotic effects of proinflammatory stimuli mainly were due to the expression of inducible NO synthase. Cyclosporin A

and FK506 inhibited partially NO synthesis. However, both NO and immunosuppressors induced apoptosis, probably through a common mechanism that involved the irreversible opening of the mitochondrial permeability transition pore. Activation of caspases 3 and 7 was observed in cells treated with high doses of NO and with moderate concentrations of immunosuppressors. The conclusion is that the cooperation between NO and immunosuppressors that induce apoptosis in PTEC might contribute to the renal toxicity observed in the course of immunosuppressive therapy.

Proximal tubular epithelial cells (PTEC) have been involved in the pathophysiology of several renal diseases, as well as in renal transplant rejection and drug-induced nephrotoxicity (1,2). These studies indicate that tubular damage in various renal diseases is dependent, at least in part, on caspase activation and induction of apoptosis, and the pathways regulating this response are a subject of intense research (3–8). Previous results showed a special sensitivity of these cells to undergo apoptosis in the course of immunosuppression with cyclosporin A (CsA) and FK506 (2,6,9). Indeed, both drugs are nephrotoxic; each produces similar histologic patterns of injury to renal tubules and preglomerular arterioles, and this toxicity is a major cause of renal allograft dysfunction. The mechanisms of CsA-induced nephrotoxicity are not fully understood, but they seem to be associated with renal hypoxia and increases in the synthesis of free radicals (10,11). In addition to this, nitric oxide (NO) participates in CsA-dependent nephrotoxicity (12,13). However, although the mechanism of NO-induced apoptosis in these cells is well established (1,14–16), the interaction between immunosuppressors and NO in terms of potentiation of apoptosis still remains elusive.

The pathways that lead to apoptosis in response to NO involve the release of mitochondrial mediators as deduced by the prevention of apoptosis using caspase inhibitors acting down-

stream in the mitochondrial signaling pathway (17,18). Constitutive expression of endothelial NO synthase (NOS-3) has been identified in epithelial cells of the kidney, including those of the proximal tubule, thick ascending limb, and inner medullar collecting duct and in interstitial cells (19). Moreover, bacterial cell wall products, such as lipopolysaccharide (LPS) and lipopeptides (TPP), and proinflammatory cytokines, such as interleukin-1 (IL-1 $\beta$ ), interferon- $\gamma$  (IFN- $\gamma$ ), and tumor necrosis factor- $\alpha$  (TNF- $\alpha$ ), are important mediators in the progression of acute renal failure, which is a frequent complication of sepsis, and exert the cytotoxic effects through the expression of the high-output NO synthase NOS-2 (20). NO and its derived metabolite peroxynitrite (ONOO<sup>-</sup>) participate in renal tubular cell injury, in the regulation of renal hemodynamics and sodium tubular transport, and in the cytotoxic mechanisms responsible for acute renal allograft rejection, where macrophages express high levels of NOS-2 (9). We recently observed that the apoptosis caused by NO in peritoneal macrophages was inhibited by treatment of the cells with CsA or with FK506, mainly through the inhibition of the expression of NOS-2 (21). In view of these results, we investigated whether immunosuppressors and NO act on apoptotic signaling in PTEC, because these cells have been described as extremely sensitive to NO and CsA to induce apoptotic death. Our data show that contrary to other cells, immunosuppressors and NO exert a synergistic action that induces apoptosis on PTEC, probably through an increase of the release of mitochondrial apoptotic mediators as reflected by the enhancement in the activity of caspases 3 and 7.

Received January 28, 2000. Accepted May 18, 2000.

Correspondence to Dr. Lisardo Bosca, Instituto de Bioquímica, Facultad de Farmacia, 28040 Madrid, Spain. Phone: +34-91-394-1853; Fax: +34-91-394-1782; E-mail: boscal@eucmax.sim.ucm.es

1046-6673/1112-2315

Journal of the American Society of Nephrology

Copyright © 2000 by the American Society of Nephrology

## Materials and Methods

### Chemicals

Chemical reagents were from Merck (Darmstadt, Germany), Roche (Mannheim, Germany), and Sigma (St. Louis, MO) and were of the

highest quality available. LPS from *Escherichia coli*, serotype 055:B5, was from Sigma. The synthetic lipopeptide S-[2,3-bis(palmitoyl)-(2-RS)-propyl]N-palmitoyl-(R)-Cys-Ser-Lys<sub>4</sub> (TPP), murine recombinant IL-1 $\beta$ , and murine recombinant TNF- $\alpha$  were from Roche. Materials and chemicals for electroporation were from Bio-Rad (Richmond, CA). Fluorescence probes were from Molecular Probes (Eugene, OR). Antibodies were from Santa Cruz Biotechnology (Santa Cruz, CA). Culture media were from BioWhittaker (Verviers, Belgium).

### Preparation of Pig Proximal Tubule Cells

Kidneys from healthy isogenic mini-pigs (Maryland strain) were removed by surgery under sterile conditions. Animals were cared for as outlined in the "Guide for the Care and Use of Laboratory Animals" (NIH publication). The kidney cortex (without medullary content) was sliced (2 mm slices) and incubated for 30 min at 37°C with collagenase (0.6 mg/ml) in Ham's-F12:Dulbecco's modified Eagle's

medium (vol:vol) (incubation medium). The digested tissue was centrifuged at  $100 \times g$  for 30 s, and the pellet was washed twice with incubation medium. The cell pellet was resuspended in 45% Percoll (10 ml of Percoll per gram of original tissue) and centrifuged at  $20,000 \times g$  for 30 min. Proximal tubular cells banded in a well-defined bottom layer that was characterized both biochemically and morphologically following previous work (22). Cells ( $1$  to  $2 \times 10^6$ ) were seeded in 6-cm dishes with incubation medium supplemented with 2.5 mM glutamine, antibiotics,  $10^{-8}$  M hydrocortisone, and 2% of complement-free fetal calf serum. Cells were maintained for 2 d with a daily change of medium and used after the third day in culture.

### Measurement of Apoptosis

Apoptosis was determined by three independent criteria: the appearance of DNA fragmentation, the release of oligonucleosomes

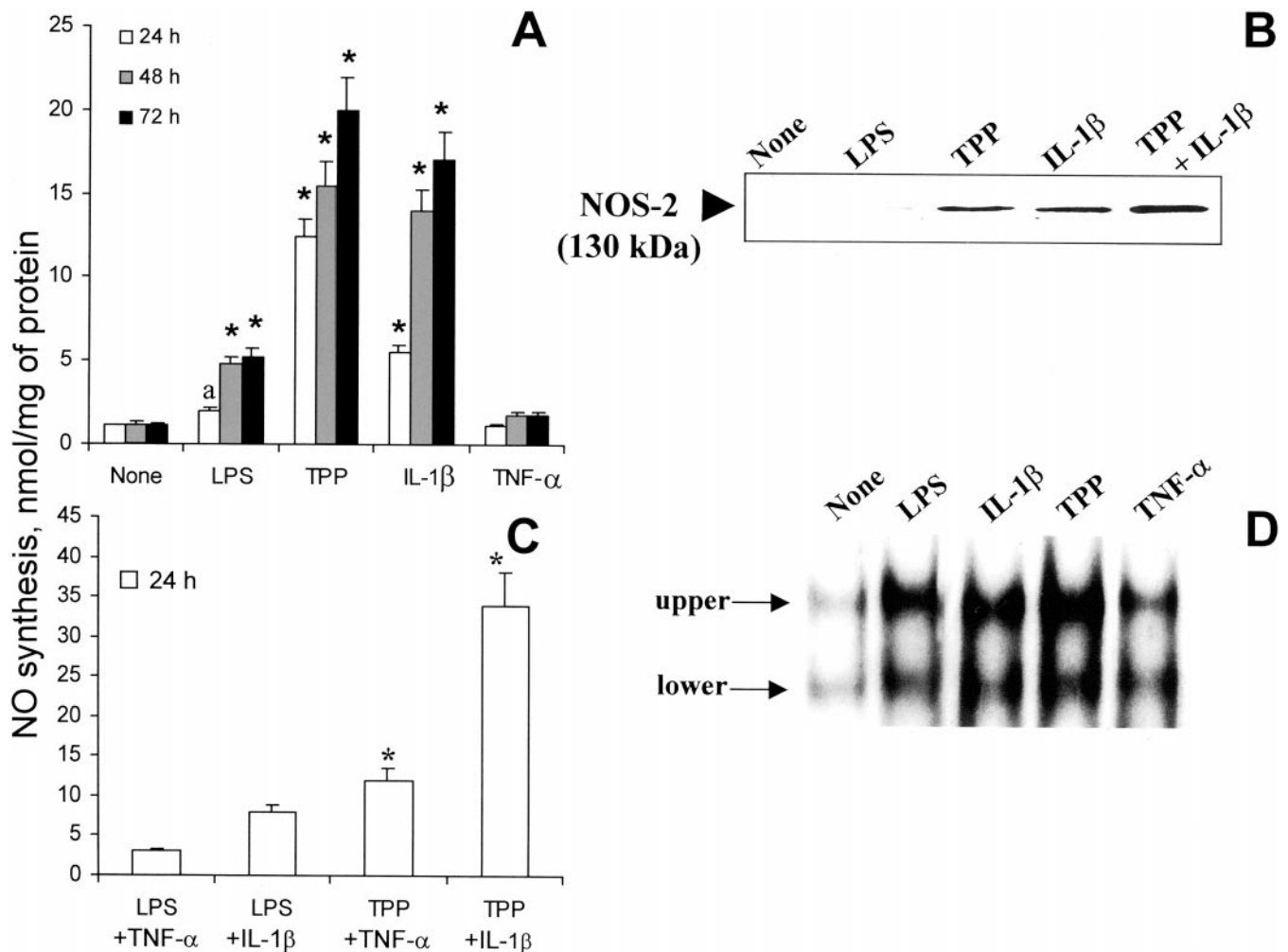


**Figure 1.** Lipopolysaccharide (LPS), tris-palmitoyl-peptide (TPP), and interleukin-1 $\beta$  (IL-1 $\beta$ ) increase nitric oxide (NO) synthesis in primary cultures of proximal tubular epithelial cells. Cells ( $2 \times 10^5$ ) were stimulated with 1  $\mu$ g/ml LPS, 5  $\mu$ g/ml TPP, 20 ng/ml murine IL-1 $\beta$ , 100 ng/ml murine tumor necrosis factor- $\alpha$  (TNF- $\alpha$ ), or combinations of these. The amount of nitrite plus nitrate was determined at the indicated times in samples of the culture medium, after reduction of nitrate to nitrite, and using Griess reagent (A and C). NOS-2 protein levels were determined at 24 h by Western blot using an antimurine-NOS-2 antibody (B). Activation of nuclear factor  $\kappa$ B (NF- $\kappa$ B) was determined by electrophoretic mobility shift assays using nuclear protein extracts from cells treated for 2 h with the indicated stimuli (D). Results show a representative experiment (B and D) and the mean  $\pm$  SEM of three experiments. a,  $P < 0.05$ ; \*,  $P < 0.01$  versus the none condition at the indicated times (A) and the LPS condition (C), respectively.

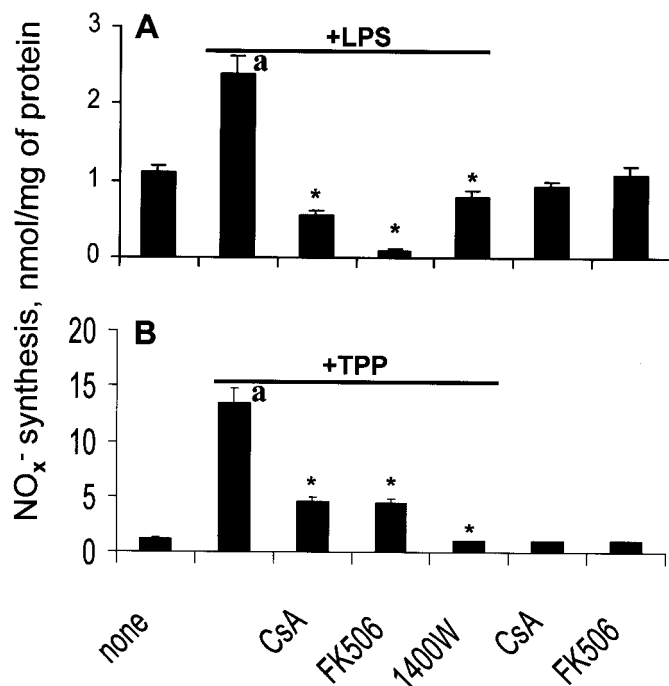


**Figure 2.** Cyclosporine A (CsA) and FK506 inhibit NO synthesis in proximal tubular epithelial cells (PTEC) stimulated with LPS or TPP. Cells were incubated for 24 h with combinations of LPS (1  $\mu$ g/ml; A) or TPP (5  $\mu$ g/ml; B), and CsA (10 nM), FK506 (10 nM), and 1400W (100  $\mu$ M). The synthesis of NO was determined by the accumulation of nitrate plus nitrite. Results show the mean  $\pm$  SEM of three experiments. \*,  $P < 0.001$  with respect to the LPS or TPP conditions; a,  $P < 0.01$  with respect to the none condition.

from the nucleus to the cytosol, and differential staining of the cells with propidium iodide (PI) and SYTO 13 followed by microscopic observation of the nuclei. Internucleosomal DNA fragmentation was analyzed by agarose gel as follows: The cell layer (1 to 2  $\times 10^6$  cells) was washed twice with phosphate-buffered saline, and the plasma membrane was lysed with 0.8 ml of 10 mM ethylenediaminetetraacetate (EDTA), 0.25% Triton X-100, 20 mM Tris-HCl (pH 8.0; 15 min at 4°C). The DNA from the total cell extract was precipitated with 70% ethanol plus 2 mM MgSO<sub>4</sub> and treated for 4 h at 55°C with 0.5 mg/ml proteinase K. After two extractions with phenol/chloroform, the DNA was analyzed in a 2% agarose gel and stained with 0.5  $\mu$ g/ml ethidium bromide (23,24). Alternatively, the lysed cells were centrifuged at 30,000  $\times g$  for 15 min to remove nuclei and mitochondria and the DNA present in the soluble fraction was analyzed using an enzyme-linked immunosorbent assay cell death kit (Boehringer) in which the histone-associated DNA fragments were detected by a sandwich-enzyme immunoassay with antihistone and anti-DNA-peroxidase antibodies. The relative degree of apoptosis was quantitatively determined by measuring the peroxidase activity at 405 nm and calculating the ratio between the enzyme activity of treated cells and the corresponding value of control cells (enrichment factor). In addition to these methods, the cells were stained *in vivo* with 0.005% of PI (red fluorescence) and 50  $\mu$ M SYTO 13 (green fluorescence; Molecular Probes). The changes in cellular morphology and the appearance of apoptotic bodies were determined by confocal microscopy.

### Preparation of Nuclear Extracts

Protein extracts were prepared following the method of Schreiber *et al.* (25), as described previously. Protein content was assayed using the Bio-Rad detergent-compatible protein reagent. All steps of cell fractionation were carried out at 4°C.

### Electrophoretic Mobility Shift Assays

The oligonucleotide sequences that correspond to the consensus nuclear factor  $\kappa$ B (NF- $\kappa$ B) binding site (nucleotides -978 to -952) 5'TGCTAGGGGGATTTCCTCTCTGT3' (26) of the murine NOS-2 promoter were used. Aliquots of 100 ng of annealed oligonucleotide were end-labeled with Klenow enzyme fragment. A total of 5  $\times 10^4$  dpm of the DNA probe were used for each binding assay of nuclear extracts as follows: 3  $\mu$ g of protein were incubated for 15 min at 4°C with the DNA and 2  $\mu$ g of poly(dI:dC), 5% glycerol, 1 mM EDTA, 100 mM KCl, 5 mM MgCl<sub>2</sub>, 1 mM dithiothreitol, and 10 mM Tris-HCl (pH 7.8) in a final volume of 15  $\mu$ l. The DNA-protein complexes were separated on native 6% polyacrylamide gels in 0.5% Tris-borate-EDTA buffer (27). Supershift assays were carried out after incubation of the nuclear extract with the antibody (0.5  $\mu$ g) for 1 h at 4°C, followed by electrophoretic mobility shift assays (EMSA). Anti-p50 (human), anti-c-Rel (human), and anti-p65 (murine) antibodies were from Santa Cruz Biotechnology.

### Analysis of Mitochondrial Transmembrane Potential by Confocal Microscopy

To measure the mitochondrial transmembrane potential ( $\Delta\Omega_m$ ), cells were incubated at 37°C for 15 min in the presence of 30 nM chloromethyl X-rosamine (CMXRos) (18), followed by immediate analysis of fluorochrome incorporation in a confocal microscope. As an internal control, labeled cells were incubated with 10  $\mu$ M of the uncoupling agent *m*-chlorophenylhydrazone carbonylcyanide (*m*-CICCP) that decreased CMXRos fluorescence (28,29). Cells were visualized using an MRC-1024 confocal microscope (Bio-Rad), and the fluorescence was acquired and electronically evaluated. Laser sharp software (Bio-Rad) was used to determine the intensity of the fluorescence per pixel.  $\Delta\Omega_m$  was calculated as percentage of the change in cell fluorescence *versus* the corresponding *m*-CICCP condition (100%).

### Analysis of Mitochondrial Swelling

Mitochondria were prepared from renal cortex by differential centrifugation in isolation medium (300 mM mannitol, 1 mM ethyleneglycol-bis[ $\beta$ -aminoethyl ether]-*N,N*[prime]-tetraacetic acid, 10 mM Tris-HCl [pH 7.4]; 1 mM PO<sub>4</sub>H<sub>2</sub>K, 0.5 mM phenylmethylsulfonyl fluoride, 0.2% bovine serum albumin and gassed with N<sub>2</sub>) and resuspended 1:1 (vol:vol) in this medium. Mitochondrial swelling was determined spectrophotometrically as described (28). The mitochondrial volume ( $\mu$ l/mg of protein) was calculated as [(1/A<sub>520 nm</sub> - 0.119)  $\times$  (protein)]/0.006. The assay was performed at 37°C under continuous stirring.

### Caspase Assay

The activity of caspases was determined in cell lysates using N-acetyl-YVAD-7-amino-4-methylcoumarin (caspase 1) and N-acetyl-DEVD-7-amino-4-methylcoumarin (caspases 3 and 7), respectively, as fluorogenic substrates and following the instructions of the supplier (PharMingen, San Diego, CA). The corresponding peptide aldehyde and z-Val-Ala-DL-Asp-fluoromethylketone (z-VAD-fmk) were used to inhibit the caspase activity *in vitro* and *in vivo*,

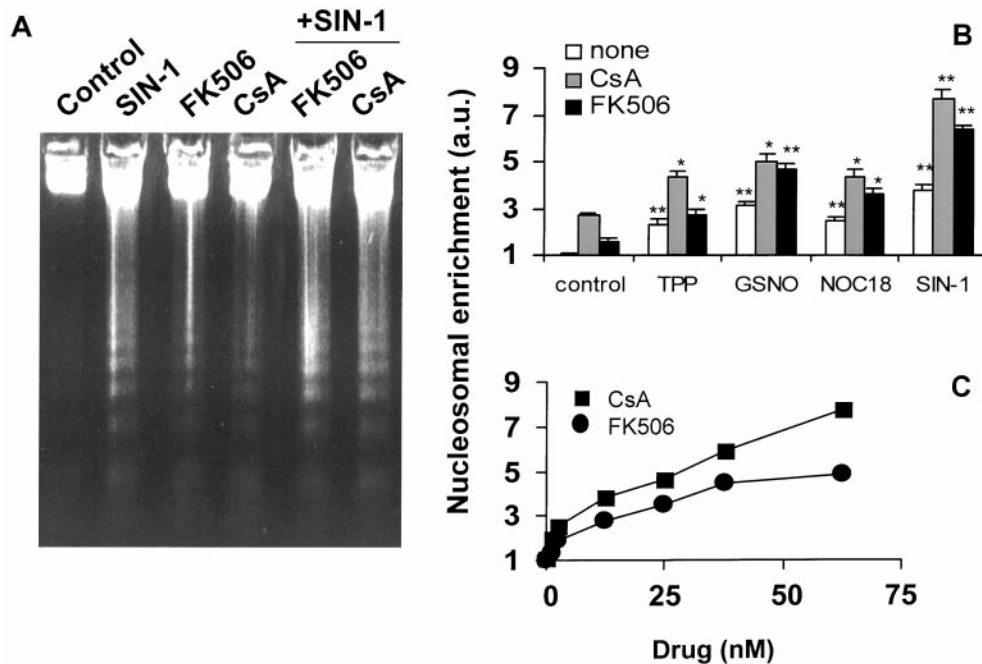


**Figure 3.** CsA and FK506 potentiate apoptosis induced by NO donors in PTEC. Cultured cells were treated for 24 h with the NO donors 3-morpholinosydnonimine (0.5 mM), 1-[2-(2-aminoethyl)-N-(2-ammonioethyl)amino]diazene-1-ium-1,2-diolate] (1 mM), and S-nitrosoglutathione (GSNO; 0.5 mM) and with the immunosuppressors CsA (10 nM) and FK506 (10 nM). Apoptosis was determined following the laddering of DNA in agarose gels (A) or determining the release of oligonucleosomal moieties from the nucleus to the cytosol using an enzyme-linked immunosorbent sandwich assay that included anti-DNA and antihistone antibodies (B and C). \*,  $P < 0.01$  and \*\*,  $P < 0.001$  with respect to the control condition.

respectively, and to ensure the specificity of the reaction. The linearity of the caspase assay was determined over a 30-min reaction period.

#### Nitrite and Nitrate Determination

NO release to the culture medium was determined spectrophotometrically by the accumulation of nitrite and nitrate as described (21). Nitrate was reduced to nitrite and determined with Griess reagent by adding sulfanilic acid and naphthylethylenediamine (1 mM in the assay). The absorbance at 548 nm was compared with a standard of  $\text{NaNO}_2$ .

#### Western Blot Analysis

The cell layers were washed twice with ice-cold phosphate-buffered saline and scraped off the dishes, and the cells collected by centrifugation. Cytosolic extracts were prepared after homogenization with ice-cold 0.3 M sucrose, 1 mM EDTA, 0.5 mM phenylmethylsulfonyl fluoride, 10  $\mu\text{g}/\text{ml}$  leupeptin, and 20 mM Tris-HCl (pH 8.0) and centrifugation for 10 min in an Eppendorf centrifuge. Aliquots of 10  $\mu\text{g}$  of the soluble protein were submitted to sodium dodecyl sulfate-polyacrylamide gel electrophoresis (10% gel) and transferred to a polyvinylidene difluoride membrane (Amersham, Bucks, UK). The amount of NOS-2 was measured using a rabbit anti-mouse NOS-2 antibody (Santa Cruz Biotechnology) that recognized a protein of the expected size (130 kD). The blot was revealed using the enhanced chemiluminescence technique (Amersham).

#### Statistical Analyses

The data shown are the mean  $\pm$  SEM of four experiments. Statistical significance was determined with *t* test for unpaired observations.  $P < 0.05$  was considered significant. In studies of Western blot

analysis, linear correlations between increasing amounts of input protein and signal intensity were observed (correlation coefficients  $>0.8$ ).

## Results

### Bacterial Cell Wall Products and IL-1 $\beta$ Promote NOS-2 Expression

Challenge of primary cultures of PTEC with LPS, the synthetic lipopeptide derived from bacterial lipoproteins TPP and IL-1 $\beta$ , promoted the expression of NOS-2 as assessed by the time-dependent accumulation of nitrate plus nitrite in the culture medium (Figure 1A) and by the immunodetection of the protein by Western blot (Figure 1B). The levels of NOS-2 in cells treated for 24 h with LPS were 6- and 3.7-fold lower than those elicited by TPP and IL-1 $\beta$ , respectively (Figure 1B). Attempts to potentiate the effect of LPS with TNF- $\alpha$ , IL-1 $\beta$ , and IFN- $\gamma$  (not shown) were ineffective, probably because these cytokines, especially IFN- $\gamma$ , were not species specific (see the "Discussion" section; Figure 1C). However, TPP induced important levels of NOS-2 and synergized with IL-1 $\beta$  (threefold increase in protein levels and enzyme activity at 24 h; Figure 1, B and C). Because NOS-2 expression requires the activation of NF- $\kappa$ B, the sequence corresponding to the  $\kappa$ B site of the murine NOS-2 promoter was used in EMSA to evaluate the engagement of this transcription factor in stimulated PTEC. As Figure 1D shows, NF- $\kappa$ B was activated upon treatment of the cells with LPS, TPP, IL-1 $\beta$ , and a high dose of



murine TNF- $\alpha$ . On analysis by supershift assays, the bands retained corresponded mainly to p50-p65 (upper band) and to p50-p50 dimers (lower band), respectively. It is interesting that LPS increased the intensity of the upper band (p50-p65 complexes) to levels similar to those elicited by TPP and IL-1 $\beta$ , although the expression of NOS-2 was lower when compared with the other bacterial stimuli TPP, suggesting the requirement of another cytokine, probably IFN- $\gamma$ , to accomplish NOS-2 expression as described for other cells (26).

The NO synthesis induced by LPS and TPP decreased significantly after treatment of the cells with 10 nM CsA and FK506 (Figure 2). To ensure that this NO synthesis was due to the expression of NOS-2, cells stimulated with LPS or TPP were incubated with the NOS-2-specific inhibitor N-[3-(aminomethyl)benzyl] acetamide (1400W) and the amount of nitrite plus nitrate was similar to that of untreated controls. Neither of the immunosuppressors influenced NO production in control cells. Concentrations of CsA higher than 100 nM were toxic for these cells as deduced by the release of lactate dehydrogenase to the extracellular medium after 24 h of culture (not shown).

#### NO, CsA, and FK506 Induce Apoptosis in PTEC

NO has been recognized as a self-sufficient molecule inducing apoptosis in various cell types (17,18,28). Indeed, treatment of PTEC with NO donors such as 3-morpholinopyridone, S-nitrosoglutathione (GSNO), and 1-[2-(2-aminoethyl)-N-(2-ammonioethyl)amino]diazene-1-ium-1,2-diolate (NOC18) induced apoptosis as determined by the appearance of a characteristic DNA ladder (Figure 3A) and by the release of DNA

oligonucleosomal moieties from the nucleus to the cytosol (Figure 3B). CsA and FK506 also promoted apoptotic death of PTEC, an effect that was potentiated in the presence of stimuli that induce NOS-2 expression (TPP) or after release of elevated concentrations of NO by NO donors (Figure 3B). The dose-dependent effect of CsA and FK506 on apoptosis is shown in Figure 3C. The half-maximal response was obtained at 20 nM and 15 nM of FK506 and CsA, respectively. This ability of CsA and FK506 to induce apoptosis in PTEC was evaluated also by confocal microscopy using PI and SYTO 13 simultaneous staining. As Figure 4 shows, CsA and FK506 induced the appearance of apoptotic bodies and chromatin condensation in PTEC, a process that was enhanced in the presence of the NO donor GSNO. A quantitative determination of the cell population exhibiting apoptotic features is shown in Table 1. Agreement was observed between the percentage of cells with apoptotic bodies (Table 1) and the relative accumulation of oligonucleosomes in the cytosol (Figure 3, B and C). Moreover, incubation of cells with the general caspase inhibitor z-VAD.fmk and with DEVD-CHO, that inhibits preferentially the downstream caspases 3 and 7, prevented the apoptosis induced by NO donors and immunosuppressors. The inhibition of apoptosis exerted by z-VAD.fmk persisted significantly up to 72 h after treatment with GSNO and CsA (Table 1). Also, other inhibitors of apoptosis, such as 3-aminobenzamide and 6(5H)phenanthridinone (30,31), were very efficient in protecting the cells from apoptosis (see the "Discussion" section). These data suggest that the apoptosis induced in PTEC by NO donors and immunosuppressors can be inhibited pharmacologically with these drugs.

A decrease of  $\Delta\Omega_m$  has been described as a common, if not causal, event in the induction of apoptosis in several cell types

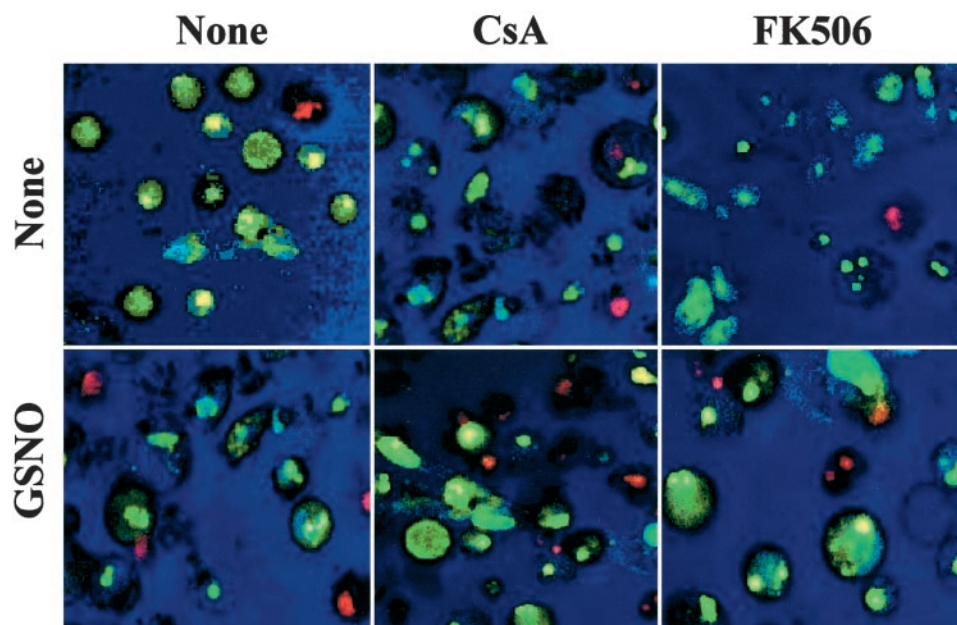


**Figure 4.** Apoptosis of PTEC treated with GSNO and immunosuppressors. Cells were incubated for 24 h with 0.5 mM GSNO, 10 nM CsA, 10 nM FK506, or combinations of these. At the end of the incubation period, the cells were stained with propidium iodide (red fluorescence), a dye excluded from viable cells that allows visualization of necrotic and early apoptotic cells, and SYTO 13 (green fluorescence), a live-cell nucleic acid stain. Apoptosis was determined by morphologic changes and by the presence of condensed DNA and apoptotic bodies in SYTO 13 stained cells. The cells were visualized using confocal microscopy.

Table 1. Inhibition of apoptosis by caspase inhibitors<sup>a</sup>

Stimuli	Apoptotic Cells (per 100)				
	None	z-VAD	DEVD-CHO	6PTD	ABZ
24 h					
none	2 ± 1	1	3 ± 2	2 ± 1	2 ± 1
TPP, 5 μg/ml	16 ± 1	8 ± 1	10 ± 1	3 ± 1	2 ± 1
IL-1β, 20 ng/ml	11 ± 2	8 ± 1	7 ± 2	3 ± 1	4 ± 1
GSNO, 500 μM	19 ± 2	7 ± 1	9 ± 1	3 ± 1	5 ± 1
CsA, 10 nM	14 ± 2	7 ± 2	6 ± 1	4 ± 1	3 ± 2
TPP + IL-1β	24 ± 3	11 ± 2	11 ± 2	5 ± 1	5 ± 1
TPP + CsA	30 ± 3	10 ± 1	11 ± 2	6 ± 1	6 ± 1
GSNO + CsA	36 ± 4	9 ± 2	9 ± 2	5 ± 1	7 ± 1
72 h					
none	3 ± 1	4 ± 1			
GSNO	25 ± 3	12 ± 3			
CsA	32 ± 4	17 ± 2			
GSNO + CsA	52 ± 6	19 ± 4			

<sup>a</sup> PTEC were treated for 24 or 72 h with the indicated stimuli in the absence or presence of the caspase inhibitors z-VAD.fmk (50 μM) and DEVD.CHO (100 μM) and with the immunosuppressors and apoptosis inhibitors 6PTD (0.5 mM) and ABZ (2 mM). The extent of apoptosis was determined by confocal microscopy observation of apoptotic bodies after staining with PI and SYTO13, as described in Figure 4. Results show the mean ± SEM of three experiments ( $n = 100$  to 120 cells). PTEC, proximal tubular epithelial cells; 6PTD, 6(5H)phenanthridinone; ABZ, 3-aminobenzamide; TPP, tris-palmitoyl-peptide; IL-1β, interleukin 1β; GSNO, S-nitrosoglutathione; CsA, cyclosporin A.

(28,29). Incubation of PTEC with CMXRos as probe for the determination of the  $\Delta\Omega_m$  showed a decrease of potential after prolonged treatment with GSNO and CsA (6 h). Simultaneous addition of GSNO and CsA did not enhance the decrease of  $\Delta\Omega_m$ , suggesting the use of a common pathway in the irreversible opening of the permeability transition pore (PT; Figure 5A). As a positive control, we determined the changes of the fluorescence produced by the uncoupling drug *m*-CICCP, which was considered as 100% of the decrease of  $\Delta\Omega_m$ . These results are compatible with a role for the fall of  $\Delta\Omega_m$  in CsA-dependent apoptosis. However, CsA has been character-

ized as an inhibitor of the PT in various cell types, at least at short periods. Indeed, this was the case, and the pore remained unchanged during the early 20 min after CsA treatment (Figure 5A), a period during which no changes in volume of isolated mitochondria incubated with succinate were observed (Figure 5B). In agreement with these data, mitochondrial swelling was observed after 25 to 30 min of incubation with succinate and CsA.

#### Activation of Caspases in PTEC

The preceding results suggest a contribution of mitochondrial signals to induction of apoptosis in PTEC cells treated

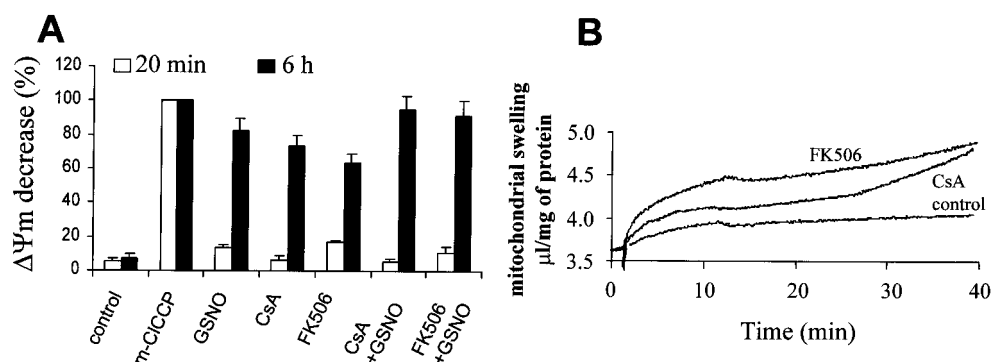


Figure 5. Effect of CsA and FK506 on  $\Delta\Omega_m$  and mitochondrial swelling in PTEC. Cells were incubated with 0.5 mM GSNO, 10 nM CsA, and 10 nM FK506, and at the indicated times the  $\Delta\Omega_m$  was measured after labeling the cells with 30 nM chloromethyl X-rosamine for 15 min at 37°C. The decrease of fluorescence of cells treated with *m*-chlorophenylhydrazone carbonyl cyanide was considered as 100% of the change in  $\Delta\Omega_m$  (A). Isolated mitochondria from PTEC were incubated with 5 mM succinate and in the presence of 10 nM CsA or 10 nM FK506. The swelling was determined spectrophotometrically (B). Results show the mean of five experiments.

with NO donors and immunosuppressors. To determine the involvement of caspases in this process, we measured the activity of DEVD-specific caspase (3 and 7), which mediates the executioner step of apoptosis, and caspase 1 (YVAD as substrate), which is more related to inflammatory mechanisms. As Figure 6 shows, DEVDase activity increased in cells that were treated with GSNO and to a lower extent in cells that were stimulated with CsA and FK506. Incubation of cells with GSNO and CsA or FK506 did not increase significantly the caspase activity induced by GSNO, suggesting the convergence in the mechanisms of caspase activation. The activity of caspase 1 remained unchanged regardless of the treatments used, indicating that this activity was not involved in the process.

## Discussion

The expression of NOS-2 and the synthesis of NO by PTEC may constitute an important event in the onset of inflammatory renal diseases. PTEC exhibit a moderate response to LPS in terms of expression of NOS-2 but are highly sensitive to the action of proinflammatory cytokines and other components of the bacterial cell wall, such as the lipoproteins (1,32). Our data show that the apoptotic effects of NO are reinforced under conditions of immunosuppression, suggesting a concerted mechanism in the induction of apoptosis. This behavior of PTEC regarding the sensitivity to NO and CsA/FK506-induced apoptosis seems to be typical of these and other epithelial cells, such as the cell lines LLC-PK1 and SH-SY5Y (30,33). Indeed, protection against apoptosis and NOS-2 expression by CsA and FK506 has been described in other cells, such as macrophages, C6 glioma cell line, and L929 fibroblasts (21,34,35).

One advantage of the experimental model used was that the cell cultures were virtually depleted of monocytes and activated T cells; therefore, the immunomodulatory molecules that

were produced after cell stimulation were synthesized mainly by PTEC. This was confirmed by the absence in unstimulated cells of NF- $\kappa$ B activity, a good sensor of inflammatory stress (36,37). The mechanisms by which CsA and FK506 promote apoptosis in PTEC are not clearly established, but mitochondrial swelling as a result of the fall of mitochondrial PT after treatment with these drugs has been observed consistently. Mitochondrial PT opening has been identified as a target of the apoptotic action of NO both in intact cells and in reconstituted systems that contain isolated mitochondria and nuclei (18,28,29). Indeed, caspase 3 activity increased in cells that were treated with GSNO, CsA, or FK506; however, absence of synergic effects was observed when PTEC cells were incubated with GSNO and CsA or FK506, suggesting the use of a common downstream apoptotic pathway. Moreover, peptide inhibitors of caspases such as zVAD-fmk and DEVD-CHO (which inhibit caspase 3 and related caspases) prevented NO and CsA/FK506-induced apoptosis in PTEC cells.

Several pathways have been proposed to explain the sensitivity of PTEC to undergo apoptosis (6). These included enhancement of oxygen radical synthesis in the ischemia-reperfusion injury (38,39). Under these conditions, poly-ADP-ribose polymerase (PARP) inhibitors proved to be effective in protecting against apoptosis (40). In agreement with these results, incubation of PTEC with PARP inhibitors 3-AB and possibly 6(5H)phenanthridinone abrogated the apoptosis induced by immunosuppressors and NO donors. The other candidate to mediate the toxic effects of NO and reactive oxygen species is peroxynitrite. Indeed, in models of LPS-induced kidney injury, an accumulation of nitrotyrosine has been detected in PTEC, and it has been proposed that protein nitration may participate in renal failure. The precise mechanism of action of peroxynitrite in these cells is not fully understood (38,41); however, it seems to involve an inhibition of the adhesion properties of the PTEC, a process lost as a result of NO and OONO synthesis (42). In this regard, removal of NO and peroxynitrite with scavengers protected efficiently against ischemia/reperfusion injury in the course of acute renal failure (12,13).

Other indirect data suggest an important role for NO in the degeneration of kidney functions, *e.g.*, supplementation of the diet with arginine increases renal injury (15). Moreover, in transgenic sickle cell mouse kidney, there is an overproduction of NO as a result of the massive expression of different forms of NOS promoting apoptosis of PTEC and renal failure (38). An enhanced NO synthesis together with the elevated accumulation of oxygen superoxide leads to formation of peroxynitrite and induction of apoptotic death of PTEC via tyrosine nitration of proteins (38). These data point to mitochondrial apoptotic signaling as one of the key factors that mediate the sensitivity of renal cells to undergo apoptosis. In agreement with this suggestion, mice that lack Bcl-2 develop polycystic kidneys and exhibit rapid renal failure (4). In addition to the mitochondrial mediators, the coexistence of Fas signaling induced by CsA and possibly by FK506 might explain the cooperative induction of apoptosis by these two pathways (43).

The data reported show a selective capacity of PTEC to

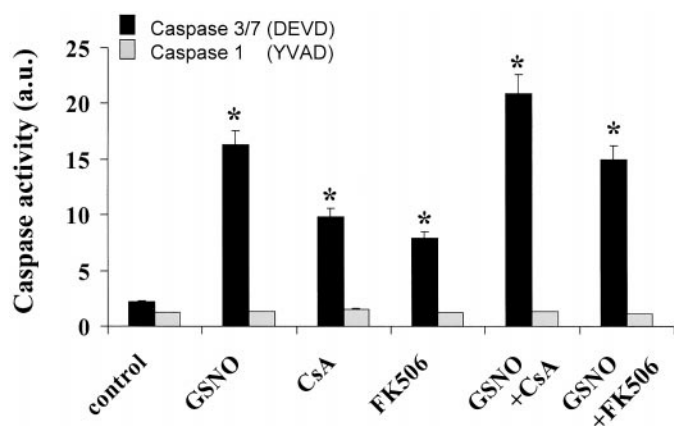


Figure 6. DEVD-caspase activity increases after treatment of PTEC with GSNO and immunosuppressors. Cells were treated for 18 h with the indicated stimuli, and cell extracts were prepared to determine the activity of caspases 3 and 7 (DEVDase activity) and caspase 1 (YVADase activity) using specific peptide substrate and inhibitors. Results show the mean  $\pm$  SEM of four experiments. \*,  $P < 0.01$  with respect to the control condition.



express NOS-2. PTEC exhibit a slight response to LPS in terms of NOS-2 expression, despite the intense activation of NF- $\kappa$ B observed by EMSA. However, challenge with proinflammatory stimuli, such as IL-1 $\beta$ , allows the synthesis of large amounts of NO that are near the range of those elicited by activated macrophages (under similar experimental conditions, the steady-state levels of NO synthesis by activated RAW cells and PTEC stimulated with lipid A plus IL-1 $\beta$  were 2 and 1.2 nmol of NO per hour and milligram of cell protein, respectively). In addition to this source of NO, the possible contribution of the infiltration of inflammatory cells such as macrophages cannot be disregarded. These data should be considered in other pathologies, such as multiorgan failure, in which treatment with inhaled NO has been proposed (44).

In summary, our results show that PTEC exhibit a marked sensitivity to apoptosis that involves the activation of DEVD-specific caspases, a process that is initiated independently by immunosuppressors and proinflammatory stimuli and that constitutes a main cause of renal injury. Evaluation of strategies that contribute to inhibition of NOS-2 expression (40), to support mitochondrial function, *e.g.*, the use of radical scavengers, or to inhibit downstream apoptotic events, *e.g.*, PARP inhibitors, might help to improve renal function under compromised situations, such as the immunosuppression that accompanies organ transplantation.

## Acknowledgments

The authors thank Dr. Alberto Alvarez from the Centro de Cito-metría de Flujo for help in the FACS analysis, O.G. Bodelón for technical help, and E. Lundin for the critical reading of the manuscript. This work was supported by grants 08/004/97 and 08/007/99 from Comunidad de Madrid, Spain.

## References

1. Markewitz BA, Michael JR, Kohan DE: Cytokine-induced expression of a nitric oxide synthase in rat renal tubule cells. *J Clin Invest* 91: 2138–2143, 1993
2. Healy E, Dempsey M, Lally C, Ryan MP: Apoptosis and necrosis: Mechanisms of cell death induced by cyclosporine A in a renal proximal tubular cell line. *Kidney Int* 54: 1955–1966, 1998
3. Conaldi PG, Biancone L, Bottelli A, Wade-Evans A, Racusen LC, Boccellino M, Orlandi V, Serra C, Camussi G, Toniolo A: HIV-1 kills renal tubular epithelial cells in vitro by triggering an apoptotic pathway involving caspase activation and Fas up-regulation. *J Clin Invest* 102: 2041–2049, 1998
4. Veis DJ, Sorenson CM, Shutter JR, Korsmeyer SJ: Bcl-2-deficient mice demonstrate fulminant lymphoid apoptosis, polycystic kidneys, and hypopigmented hair. *Cell* 75: 229–240, 1993
5. Levine JS, Koh JS, Triaca V, Lieberthal W: Lysophosphatidic acid: A novel growth and survival factor for renal proximal tubular cells. *Am J Physiol* 273: F575–F585, 1997
6. Ortiz A, Lorz C, Catalan M, Coca S, Egido J: Cyclosporine A induces apoptosis in murine tubular epithelial cells: Role of caspases. *Kidney Int Suppl* 68: S25–S29, 1998
7. Ortiz A, Lorz C, Egido J: New kids in the block: The role of FasL and Fas in kidney damage. *J Nephrol* 12: 150–158, 1999
8. Edelstein CL, Shi Y, Schrier RW: Role of caspases in hypoxia-induced necrosis of rat renal proximal tubules. *J Am Soc Nephrol* 10: 1940–1949, 1999
9. Romagnani P, Pupilli C, Lasagni L, Baccari MC, Bellini F, Amorosi A, Bertoni E, Serio M: Inducible nitric oxide synthase expression in vascular and glomerular structures of human chronic allograft nephropathy. *J Pathol* 187: 345–350, 1999
10. Zhong Z, Connor HD, Yin M, Moss N, Mason RP, Bunzendahl H, Forman DT, Thurman RG: Dietary glycine and renal denervation prevents cyclosporin A-induced hydroxyl radical production in rat kidney. *Mol Pharmacol* 56: 455–463, 1999
11. Kumar KV, Naidu MU, Shifow AA, Prayag A, Ratnakar KS: Melatonin: An antioxidant protects against cyclosporine-induced nephrotoxicity. *Transplantation* 67: 1065–1068, 1999
12. Paller MS, Weber K, Patten M: Nitric oxide-mediated renal epithelial cell injury during hypoxia and reoxygenation. *Ren Fail* 20: 459–469, 1998
13. Yu L, Gengaro PE, Niederberger M, Burke TJ, Schrier RW: Nitric oxide: A mediator in rat tubular hypoxia/reoxygenation injury. *Proc Natl Acad Sci USA* 91: 1691–1695, 1994
14. Bobadilla NA, Gamba G, Tapia E, Garcia-Torres R, Bolio A, Lopez-Zetina P, Herrera-Acosta J: Role of NO in cyclosporin nephrotoxicity: Effects of chronic NO inhibition and NO synthases gene expression. *Am J Physiol* 274: F791–F798, 1998
15. De Nicola L, Thomson SC, Wead LM, Brown MR, Gabbai FB: Arginine feeding modifies cyclosporine nephrotoxicity in rats. *J Clin Invest* 92: 1859–1865, 1993
16. Messmer UK, Briner VA, Pfeilschifter J: Tumor necrosis factor- $\alpha$  and lipopolysaccharide induce apoptotic cell death in bovine glomerular endothelial cells. *Kidney Int* 55: 2322–2337, 1999
17. Bosca L, Hortelano S: Mechanisms of nitric oxide-dependent apoptosis: Involvement of mitochondrial mediators. *Cell Signal* 11: 239–244, 1999
18. Hortelano S, Alvarez AM, Bosca L: Nitric oxide induces tyrosine nitration and release of cytochrome c preceding an increase of mitochondrial transmembrane potential in macrophages. *FASEB J* 13: 2311–2317, 1999
19. Haynes WG, Hand MF, Dockrell ME, Eadington DW, Lee MR, Hussein Z, Benjamin N, Webb DJ: Physiological role of nitric oxide in regulation of renal function in humans. *Am J Physiol* 272: F364–F371, 1997
20. Glynne PA, Evans TJ: Inflammatory cytokines induce apoptotic and necrotic cell shedding from human proximal tubular epithelial cell monolayers. *Kidney Int* 55: 2573–2597, 1999
21. Hortelano S, Lopez-Collazo E, Bosca L: Protective effect of cyclosporin A and FK506 from nitric oxide-dependent apoptosis in activated macrophages. *Br J Pharmacol* 126: 1139–1146, 1999
22. Tejedor A, Noel J, Vinay P, Boulanger Y, Gougoux A: Characterization and metabolism of canine proximal tubules, thick ascending limbs, and collecting ducts in suspension. *Can J Physiol Pharmacol* 66: 997–1009, 1988
23. Genaro AM, Hortelano S, Alvarez A, Martinez C, Bosca L: Splenic B lymphocyte programmed cell death is prevented by nitric oxide release through mechanisms involving sustained Bcl-2 levels. *J Clin Invest* 95: 1884–1890, 1995
24. Hortelano S, Bosca L: 6-Mercaptopurine decreases the Bcl-2/Bax ratio and induces apoptosis in activated splenic B lymphocytes. *Mol Pharmacol* 51: 414–421, 1997
25. Schreiber E, Matthias P, Muller MM, Schaffner W: Rapid detection of octamer binding proteins with ‘mini-extracts’, prepared from a small number of cells. *Nucleic Acids Res* 17: 6419, 1989



26. Xie QW, Whisnant R, Nathan C: Promoter of the mouse gene encoding calcium-independent nitric oxide synthase confers inducibility by interferon  $\gamma$  and bacterial lipopolysaccharide. *J Exp Med* 177: 1779–1784, 1993
27. Velasco M, Diaz-Guerra MJ, Martin-Sanz P, Alvarez A, Bosca L: Rapid up-regulation of I $\kappa$ B $\beta$  and abrogation of NF- $\kappa$ B activity in peritoneal macrophages stimulated with lipopolysaccharide. *J Biol Chem* 272: 23025–23030, 1997
28. Hortelano S, Dallaporta B, Zamzami N, Hirsch T, Susin SA, Marzo I, Bosca L, Kroemer G: Nitric oxide induces apoptosis via triggering mitochondrial permeability transition. *FEBS Lett* 410: 373–377, 1997
29. Kroemer G, Zamzami N, Susin SA: Mitochondrial control of apoptosis. *Immunol Today* 18 : 44–51, 1997
30. Filipovic DM, Meng X, Reeves WB: Inhibition of PARP prevents oxidant-induced necrosis but not apoptosis in LLC-PK1 cells. *Am J Physiol* 277: F428–F436, 1999
31. Richardson DS, Allen PD, Kelsey SM, Newland AC: Effects of PARP inhibition on drug and Fas-induced apoptosis in leukaemic cells. *Adv Exp Med Biol* 457: 267–279, 1999
32. Kabore AF, Denis M, Bergeron MG: Association of nitric oxide production by kidney proximal tubular cells in response to lipopolysaccharide and cytokines with cellular damage. *Antimicrob Agents Chemother* 41: 557–562, 1997
33. Oh-hashii K, Maruyama W, Yi H, Takahashi T, Naoi M, Isobe K: Mitogen-activated protein kinase pathway mediates peroxynitrite-induced apoptosis in human dopaminergic neuroblastoma SH-SY5Y cells. *Biochem Biophys Res Commun* 263: 504–509, 1999
34. Trajkovic V, Badovinac V, Jankovic V, Samardzic T, Maksimovic D, Popadic D: Cyclosporin A suppresses the induction of nitric oxide synthesis in interferon- $\gamma$ -treated L929 fibroblasts. *Scand J Immunol* 49: 126–130, 1999
35. Trajkovic V, Badovinac V, Jankovic V, Mostarica S : Cyclosporin A inhibits activation of inducible nitric oxide synthase in C6 glioma cell line. *Brain Res* 816: 92–98, 1999
36. Rangan GK, Wang Y, Tay YC, Harris DC: Inhibition of NF- $\kappa$ B activation reduces cortical tubulointerstitial injury in proteinuric rats. *Kidney Int* 56: 118–134, 1999
37. Mercurio F, Manning AM: Multiple signals converging on NF- $\kappa$ B. *Curr Opin Cell Biol* 11: 226–232, 1998
38. Bank N, Kiroycheva M, Ahmed F, Anthony GM, Fabry ME, Nagel RL, Singhal PC: Peroxynitrite formation and apoptosis in transgenic sickle cell mouse kidneys. *Kidney Int* 54: 1520–1528, 1998
39. Navarro-Antolin J, Hernandez-Perera O, Lopez-Ongil S, Rodriguez-Puyol M, Rodriguez-Puyol D, Lamas S: CsA and FK506 up-regulate eNOS expression: Role of reactive oxygen species and AP-1. *Kidney Int Suppl* 68: S20–S24, 1998
40. Chatterjee PK, Cuzzocrea S, Thiemermann C: Inhibitors of poly (ADP-ribose) synthetase protect rat proximal tubular cells against oxidant stress. *Kidney Int* 56: 973–984, 1999
41. Bian K, Davis K, Kuret J, Binder L, Murad F: Nitrotyrosine formation with endotoxin-induced kidney injury detected by immunohistochemistry. *Am J Physiol* 277: F33–F40, 1999
42. Wangsiripaisan A, Gengaro PE, Nemenoff RA, Ling H, Edelstein CL, Schrier RW: Effect of nitric oxide donors on renal tubular epithelial cell-matrix adhesion. *Kidney Int* 55: 2281–2288, 1999
43. Boonstra JG, van der Woude FJ, Wever PC, Laterveer JC, Daha MR, van Kooten C: Expression and function of Fas (CD95) on human renal tubular epithelial cells. *J Am Soc Nephrol* 8: 1517–1524, 1997
44. Karima R, Matsumoto S, Higashi H, Matsushima K: The molecular pathogenesis of endotoxic shock and organ failure. *Mol Med Today* 5: 123–132, 1999